

Methods for Investigating the Influence of Self-Induced Electromagnetic Emission of Electric Propulsions Upon the Sensitivity Characteristics of Onboard Radio Systems of Spacecrafts**

A.P.Plokhikh, N.A.Vazhenin, G.V.Soganova
Research Institute of Applied Mechanics and Electrodynamics (RIAME)
P.O.Box 43
Moscow 125080
Russia
7 (095) 158-0020
riame@sokol.ru

IEPC-01-257

The paper is devoted to the methodological problems of analysis for the influence of electromagnetic emission of electric propulsions (EP) upon the sensitivity characteristics of onboard radio systems. Complex approach is discussed that describes the radio channel and EP as a single electrodynamic system. Theoretical and test procedures are presented for assessing the real sensitivity of radio reception paths at a presence of operating EP. Recommendations are given on the EP integration with the spacecraft radio systems.

Introduction

Analysis of test results obtained while studying the characteristics of self emission produced by electric propulsions (EP) shows that in general case the recorded emission spectrum level is within a rather broad frequency band (from 10 kHz to 40 GHz), while the emission processes themselves are of definitely pronounced random chaotic nature and are the processes unstationary in time in general case [1], [2]. Taking into account that EP's are currently considered as the main engines for securing the orientation and orbit correction for the modern communications satellites, and that the traffic frequencies of repeater Earth-board channels are within the ranges of 5-6 GHz and 14-15 GHz, studies on defining the EP influence upon the characteristics of onboard radio systems are rather actual.

In spite of the fact that the above problem is not a new one, authors state that there is practically no

systematic approach currently to the designing of data radio channels operating under the EP active interference. As a rule, this is connected with the fact that the EP designers limit themselves by meeting the requirements of electromagnetic compatibility (EMC) standards for the extra-bandpass interference, MIL-STD-461B for example (which prescribes limitation of interference level in spectrum using the criterion of radioelectronic equipment unfailure as a result of interference effect only) and indicate this in the EP specification. Fig. 1 shows an example of comparison for the self emission of EP of SPT-100 type and the requirements of standards for the communications satellites [3].

Designers of radio receiving equipment should in their turn take into account the contribution of EP interferences appearing in the radio channel bandwidth, but as a rule such data is absent. As a result, a conclusion is made on the basis of meeting

* Presented as Paper IEPC-01-257 at the 27th International Electric Propulsion Conference, Pasadena, CA, 15-19 October, 2001.

† Copyright © 2001 by RIAME. Published by the Electric Rocket Propulsion Society with permission.

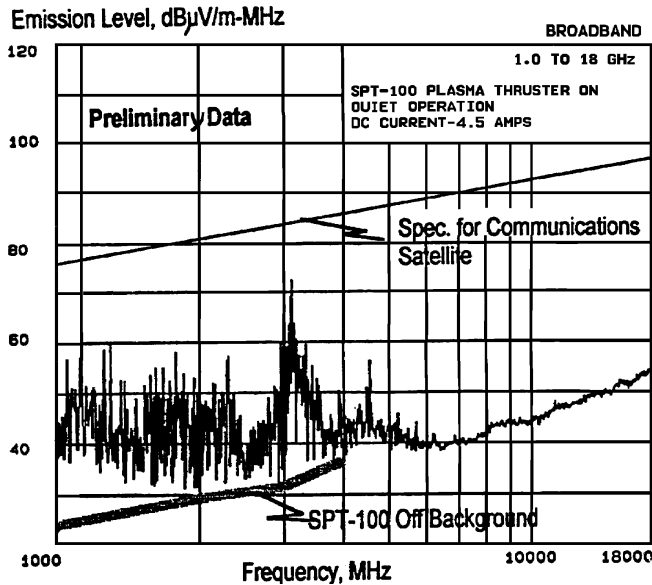


Fig.1.

the requirements of EMC standard that such interferences may be neglected. However, under definite conditions, EP bandpass interference may cause failures in the onboard radio complex operation, in spite of the fact that its level may be substantially lower than the indicated in the EMC standards. This problem becomes especially actual when designing the communication radio links for the interplanet spacecrafts equipped with sustainer EP's.

The problem of realizing the systematic approach to the designing of EP and onboard radio complex as a single electrodynamic system is stated in this paper for the first time. This approach is based on the methods of studying the influence of EP self emission on the sensitivity characteristics of the onboard radio complex receiving channels, developed by the authors.

Such parameters as sensitivity of onboard radio systems limited by noises P_{s0} (minimum signal level at the input securing the given signal-to-noise ratio h_0 at the output), and noise factor K_n with noise temperature T_n , connected functionally with it are considered as parameters characterizing the EP influence upon the operation of onboard radio systems. This is connected with the fact that for a classic radio section sensitivity, noise factor and noise temperature are the main parameters, which are calculated, measured and presented in the corresponding specification. Knowledge of these parameters allows unambiguous defining for the energetic potential of any radio link,

and thus its maximum range. The effect of EP broadband interferences appearing in the bandwidth of radio section worsens naturally its sensitivity in relation to the valid signal. So, on the basis of variation in sensitivity (noise factor, noise temperature) of radio section in the modes with operating and non-operating EP it is possible not only to define the degree of EP influence upon the operation of onboard radio systems, but to formulate the requirements to the effective interference characteristics of EP for providing the efficient operation of perspective radio systems.

Methods for Describing the Radio System Noise Immunity

Reception Path

Let's represent the reception path in a form of an equivalent linear two-port (Fig. 2). The following noises are considered as the main ones: intrinsic noises of receiver path, intrinsic noises of antenna feeder, and noises generated by EP at the receiver radio path input. In this case, the reception path is put in its input under the matched load R_{AF} (R_{AF} value is equal to the input antenna feeder resistance), while in its output it is put under the matched load R_{out} . Both loads are under the temperature $T_0=293$ K. It is assumed that all noise signals referred to the two-port input may be accurately enough presented within the radio path bandwidth as Gaussian white noise with the given spectral density. We shall assess the reception

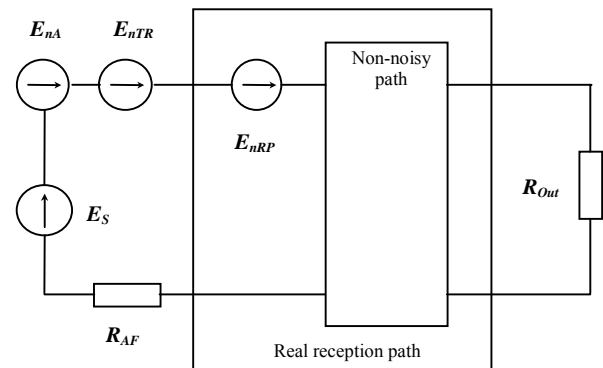


Fig.2. Reception path equivalent circuit.

E_S - e.m.f. of the valid signal at the reception radio path input; E_{nAF} - e.m.f. of the intrinsic noise signal of antenna feeder at the input of reception radio path; E_{nTR} - e.m.f. of the thruster noise signal at the reception radio path input; E_{nRP} - e.m.f. of the intrinsic noise of the reception radio path referred to its input; and R_{AF} is the antenna feeder resistance.

path noise properties via the noise factor K_N showing the variation of signal-to-noise ratio h_0 at the two-port output relative to the signal-to noise ratio h_1 at its input (in times), or to which extent the power of noise at the real two-port output exceeds the power of noise at the output of non-noisy (ideal) two-port operating under the same conditions.

$$K_N = \frac{h_1}{h_0}, \quad (1)$$

First of all, let's study the situation when EP is OFF, and intrinsic noises of antenna feeder section may be neglected in comparison to the intrinsic noises of radio reception path. For the case of ultimate sensitivity ($h_0=1$), the input signal minimum power is defined by the noise factor K_N (taking the reception path intrinsic noises into account) and by the power of thermal noise at the reception path input; resistance R_{AF} being under the temperature $T = T_0$ is the source of these noises.

$$P_{S0} = K_N k T_0 \Delta f, \quad (2)$$

where Δf is an effective noise band of radio path defined by the following expression:

$$\Delta f = \int_0^{\infty} H_{RP}^2(f) df, \quad (3)$$

where $H_{RP}(f)$ - normalized frequency response of the reception path.

As it is seen from (2), power of the thermal source noise is unambiguously defined by its physical temperature. For the non-thermal noise sources, it is convenient to introduce a concept of equivalent noise temperature T_n that is defined by the temperature of uniformly heated resistor, the noise power spectral density of which is equal to the spectral density of the noise power for the studied source. Thus, its own equivalent noise temperature may be put into correspondence to all noise sources presented in Fig. 2. In this case, in contrast to the noise factor, noise temperature of reception path characterizes it independently on the sources of external additional noises at the input. From this point of view, it is a more objective characteristic for the reception path than the noise factor. This is especially essential for the reception paths with the noise factors being close to one. In this case, parameter "noise factor" starts to lose its easiness to be interpreted even when the noises of input load are known exactly. From the other hand, it should be noted that T_n measurement requires

more complicated methods than K_N measurement. Relation between the noise factor of reception path and its equivalent temperature is defined by the following expression:

$$K_N = 1 + \frac{T_{RP}}{T_0}, \quad (4)$$

where K_N - reception path noise factor, T_{RP} - equivalent noise temperature of the reception path. This noise factor is called standard, because it is measured at the input load temperature $T = T_0$.

Let's study the situation now when EP is "ON" and its noise emission is within the main and side lobes of the receiving antenna. Taking into account the equivalent noise temperatures of all above sources, it is possible to write an expression for the "real" or "working" noise factor K_{NR} :

$$K_{NR} = 1 + \frac{T_{AF} + T_{TR} + T_{RP}}{T_0}, \quad (5)$$

where T_{AF} is an equivalent noise temperature of the antenna feeder noise source at the reception path input and T_{TR} is an equivalent noise temperature of the thruster noise source at the reception path input.

In this case, real ultimate sensitivity of the radio path is defined by the following expression:

$$P_{SR} = K_{NR} k T_0 \Delta f, \quad (6)$$

Ultimate sensitivity degradation due to additional noises may be assessed using the formulae (2) and (6):

$$\frac{P_{SR}}{P_{S0}} = \frac{K_{NR}}{K_N} \quad (7)$$

By introducing the notion of "relative equivalent noise temperature" of external noises coming via the antenna feeder to the reception path input T^* that is:

$$T^* = \frac{T_{AF} + T_{TR}}{T_0}, \quad (8)$$

we may transform (5) to the following form:

$$K_{NR} = K_N + T^* \quad (9)$$

With this, (7) is of the following form:

$$\frac{P_{SR}}{P_{S0}} = 1 + \frac{T^*}{K_N} \quad (10)$$

Thus, we come to an evident result that the reception path sensitivity degradation (at the fixed standard noise factor K_N) depends linearly on the relative

equivalent noise temperature of the external noise sources at the reception path input T^* .

It is now easy to make a transform from the reception path ultimate sensitivity to the radio link action range and its variation due to additional noises of input load:

$$\frac{R_R}{R_0} = \left(1 + \frac{T^*}{K_N}\right)^{-\frac{1}{2}}, \quad (11)$$

where R_0 is the radio link action range at $T_{AF} + T_{TR} = 0$ and R_R is the radio link action range in view of real values $T_{AF} + T_{TR}$.

Fig. 3 shows the variation of radio link relative range as a function of relation T^*/K_N . As it is obvious from the plot, at $T^* = 3K_N$ already the radio link action range drops twice. Taking into account that in real and perspective radio links the intrinsic noise factor is rather small and is close to 1, contribution of even unsubstantial external noise may become rather perceptible for the radio link energetic potential.

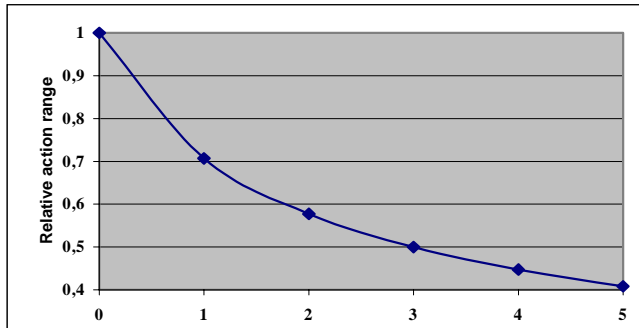


Fig.3.

Let's make the above clear, using the test data presented in Fig. 1. Comparison of the EP noise signal average value in the antenna aperture (40 dB $\mu\text{V}/\text{m}\cdot\text{MHz}$) and the background level when the thruster is "ON" (30 dB $\mu\text{V}/\text{m}\cdot\text{MHz}$) shows a 10-times excess in power (the values correspond to the frequency range of 2-3 GHz). In this case, formulae (7) and (9) allow defining that $T^* \approx 9K_N$. Then, it follows from (11), that with the operating thruster the radio link range is 0.316 of the maximum one. In this example, parameters of the EP noise emission were specially chosen to be in the range of relatively low frequencies, where the emission is maximum. Under real conditions, the most part of radio links operates at higher frequencies, where the effect may be weaker. Nevertheless, the above example definitely shows that

the electromagnetic compatibility standards are not sufficient when assessing the EP noise effect upon the spacecraft radio systems, and development of additional methods and means is required, which are presented below.

Antenna Feeder Section

The above study was based on referring the equivalent noise temperatures of all noise sources to the reception path input. With this, the effect of antenna feeder section and outer noises was taken into account in terms of the matched resistance R_{AF} , equivalent noise temperature T_{AF} , and equivalent noise temperature of external noises T_{TR} . Such approach is valid, but it does not describe the peculiarities of external noise passing through the real antenna feeder, while in some cases this is rather important. Let's analyze the structure of typical antenna feeder section comprising the receiving antenna and matched feeder connecting antenna with the receiver input. Antenna and feeder are characterized by intrinsic equivalent noise temperatures T_A and T_F .

The antenna intrinsic equivalent noise temperature T_A depends on the losses in it and may be defined by the following formula:

$$T_A = (1 - \eta_A) T_a \quad (12)$$

where T_a is the antenna temperature in Kelvin, and η_A is its efficiency.

For real antennas, T_A value is several Kelvins or some tens of Kelvins as a rule, and it drops with the wave length growth.

When external noises (noises generated by EP, in our case) reach antenna, they form a noise source at its output, characterized by the following equivalent noise temperature:

$$T_{TR1} = \frac{1}{4\pi} \int_{4\pi} T_{TR}(\theta, \varphi) D(\theta, \varphi) \sin \theta d\theta d\varphi \quad (13)$$

where $D(\theta, \varphi)$ – antenna directive gain; $T_{TR}(\theta, \varphi)$ – distribution function for the EP equivalent noise temperature in the antenna environment; θ, φ – spherical angular coordinates (sphere center is in the point of antenna location).

Expression (13) shows that T_{TR1} is defined by all EP external noises reaching both along the main, and side lobes of the receiving antenna directivity pattern.

Taking into account that EP is characterized by its own angular directivity for the noise emission, real mutual orientation of EP and receiving antenna symmetry axes is important.

The total equivalent noise temperature T_2 at the antenna output is:

$$T_2 = (1-\eta_A)T_a + \eta_A T_{TRI} \quad (14)$$

The transmission line (feeder) noises are added to the antenna noises at the receiver input. Total equivalent noise temperature at the antenna feeder output with the matched antenna and receiver is:

$$T_\Sigma = [(1-\eta_A)T_a + \eta_A T_{TRI}] \eta_F + (1-\eta_F) T_F, \quad (15)$$

where η_F is the feeder efficiency.

Presence of cross-polarization in antenna and of the shadowing obstacles in the aperture (feeder) causes additional T_Σ growth. If we use the detailed presentation of (15), then for the succession of results it is necessary to substitute $T_{AF} + T_{TR}$ by T_Σ in (8)-(11).

It is necessary to note that direct use of (13) for T_{TR} determination is difficult, because distribution of $T_{TR}(\theta, \varphi)$ in the antenna environment is unknown, as a rule. In other words, standard spatial patterns of the noise emission distribution for different EP types within the used frequency ranges are currently absent. Nevertheless, for the rough T_{TRI} estimate, it is possible to use measurement data for the electromagnetic compatibility of EP, presented in Fig. 1, for example. To do so, let's choose the noise electric field intensity at some fixed frequency and convert it into the absolute value E in V/m-MHz units. Thus, the electric field intensity is known for the EP noise signal at the known distance, given frequency, within the frequency range of 1 MHz.

With the E knowledge in the pick-up antenna aperture, it is easy to define the corresponding power flow density Π :

$$\Pi = E^2/2\rho, \quad (16)$$

where ρ is the free space resistance ($\rho = 120\pi$ Ohm).

In this case, noise power at the antenna output at the given central frequency within the frequency range of 1 MHz is:

$$P = \Pi A_{\text{eff}}, \quad (17)$$

where A_{eff} is an effective area of pick-up antenna (the known value).

Assume that η_A and η_F are close to 1, i.e. that the whole power received in the antenna aperture is transmitted to the antenna feeder output without losses. Using (9) and taking the fact into account that intrinsic thermal noises will be present at the antenna output also, it is possible to write the following expression:

$$T^* \approx \frac{T_{TR}}{T_0} = \frac{P}{kT_0}, \quad (18)$$

where $k = 1.38 \cdot 10^{-23}$ W/Hz-degree and it is taken into account that $T_{TRI} = T_{TR}$.

Accuracy of such calculations is not high, because the results presented in Fig. 1 were obtained for the exact geometry of EP and pick-up antenna mutual location and may not be generalized.

Thus, accurate estimate for the EP influence upon the sensitivity characteristics of onboard radio systems is not possible without joint test studies for the noise characteristics of both thrusters and radio systems, so let's study the main metrologic bases for the measurement of noise characteristics of different noise sources.

Methods for Measuring the Noise Factor and Noise Temperature

Noise factor (noise temperature) measurement is an independent metrologic problem, and final results depend on its correct solving. As a rule, all known methods used for measuring the noise factor (noise temperature) are reduced to comparison of the device intrinsic noise power and the power of noise generator, calibrated in advance [6].

Peculiarities of noise measurements are in the following:

- There is a random component in the error of measuring the noise process parameters even under the condition of using the ideal measuring equipment (it is defined by the given time period of averaging);
- Noise signal with practically any distribution law is characterized by a large relation between the amplitude and effective values (that is why a

requirement of securing the broadened dynamic range is imposed for the measuring equipment);

- While measuring the sensitivity of radio receiving devices, the level of calibration generator signals becomes comparable to the measuring equipment noise level (while measuring low noise signals this requires the use of special methods for extracting low signals against intensive noises of measuring equipment, such as compensation, correlation and modulation methods for example).

Let's study the specifics of the noise factor measurement using the modulation method, for example, which is based on the separate indication of the noise power spectral density for the standard noise generator and of the spectral density of intrinsic noise power at the reception path output. There are several varieties of the modulation method.

Noise Factor Measuring by the Method of Two Readings

Fig. 4(a) shows the functional diagram for the noise measuring device using the method of two readings. In this case, the amplitude modulator 3 (based on a waveguide section with pin-diode, for example) is connected to the receiving section 2 output. This amplitude modulator is modulated according to the meander law by the control voltage from the reference generator 5. Measuring receiver 4 comprises a synchronous detector synchronized by reference generator 5, and because of this it reacts to the varying component of signals coming to its input only. Measuring receiver 4 comprises linear amplifiers and a square-law detector. Thus, the indications α of the measuring receiver output device are proportional to the relative noise power spectral density. Two readings are recorded during measurements: α_1 - when the noise generator and reception path are "ON"; α_2 - when the noise generator is "OFF" and reception path is "ON".

It is easy to show that:

$$\alpha_1 = k [(G + K_N) K_U - 1], \quad G = \frac{G_{GN} - kT_0}{kT_0}, \quad (19)$$

where k - proportionality coefficient; K_U - reception path gain factor; G_{GN} - spectral density of the noise generator power, and:

$$\alpha_2 = k(K_N K_U - 1) \quad (20)$$

By introducing the relation of readings $n = \alpha_1/\alpha_2$, it is

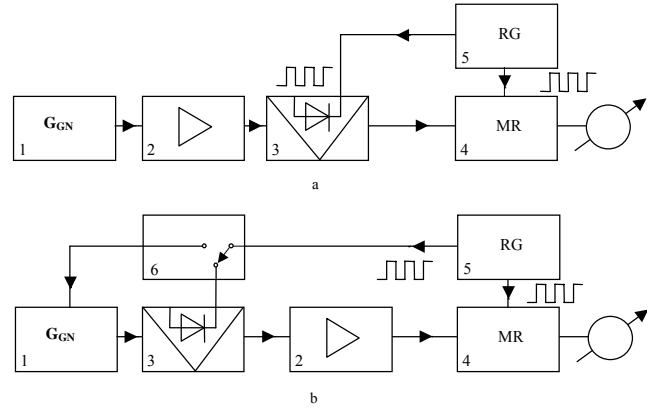


Fig. 4.

- 1- standard noise generator; 2- radio reception path; 3 - microwave modulator; 4- modulation measuring receiver (MR); 5- reference generator (RG); 6- switch.

possible to write an expression for the measured noise factor:

$$K_N = \frac{G}{n - 1} + \frac{1}{K_U}, \quad (21)$$

Taking into account that the real reception path gain factor $K_U \gg 1$, it is possible to neglect the second term in (21). It should be noted that this method has a disadvantage consisting of unlinear relation between the device readings and the measured value.

Noise Factor Measurement by the Method of Linear Scale.

The structure of metering device realizing this method is presented in Fig 4 (b). The measurement process consists of two stages: "calibration" and "measurement". During the "calibration", the switch 6 connects the reference generator 5 output to the noise generator 1 input, and its power is modulated in accordance with the meander law. In this case, measuring receiver reacts to the signal from the noise generator 1 only. During the "measurement" stage, the switch 6 connects the reference generator 5 output to the modulator 3 input that modulates the intrinsic noise of reception path 2, cutting it off periodically on the input. In this mode the noise generator is "OFF", and the measuring receiver 4 reacts to the signal of the reception path intrinsic noise only. The measuring device reading during the "calibration" is defined by the following expression:

$$\alpha_1 = kK_U G \quad (22)$$

Reading in the "measurement" mode is:

$$\alpha_2 = k(K_N K_U - 1) \quad (23)$$

Presence of correction member (-1 in brackets) is explained by the fact that when the reception path is cut off, noise temperature at its output does not comes to absolute zero, but remains to be close to T_0 .

It follows from (22) and (23) that:

$$\alpha_2 = \frac{\alpha_1}{G} \left(K_N - \frac{1}{K_U} \right) \quad (24)$$

If deviation α_1 of the output device is set to be numerically equal to G, then:

$$\alpha_2 = K_N - \frac{1}{K_U}, K_N = \alpha_2 + \frac{1}{K_U} \quad (25)$$

In view of the inequality $K_U \gg 1$, we obtain that $K_N \approx \alpha_2$. This method is called “the method of linear scale” on the basis of this.

Noise Temperature Measurement at the Antenna Feeder Output

On the basis of the “linear scale method” it is possible to propose a variant for measuring the noise temperature at the antenna feeder output by measuring the relation between the powers of noises coming first from the studied noise source with equivalent noise temperature T_{AF} , and then from the reference noise source with the equivalent noise temperature T_G . It is supposed in this case that the outer noises are absent and that the intrinsic equivalent noise temperature of the antenna feeder only is measured. The functional diagram for these measurements is presented in Fig. 5. We have the following power relation at $K_U \gg 1$:

$$n = \frac{T_{AF} + T_{RP}}{T_G} \quad (26)$$

It follows from this that:

$$T_{AF} = nT_G - T_{RP} \quad (27)$$

The principal possibility to measure the equivalent noise temperature at the antenna feeder output follows from (27). It is necessary to know for this the intrinsic equivalent noise temperature of the reception path T_{RP} that may be defined using the known noise factor K_N or measured by the above methods.

Expression (27) may be also generalized to the case of the outer noise presence in the antenna aperture, produced by EP, for example. Then, having measured the total equivalent noise temperature T_Σ at the antenna feeder output, it is possible to calculate the equivalent noise temperature of EP in the antenna

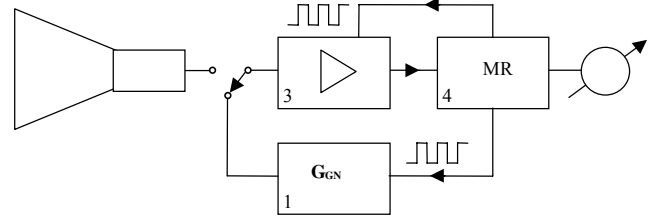


Fig.5.

aperture taking (15) into account (it is assumed that η_A , η_F and T_a are known or may be measured):

$$T_{TR1} = \frac{T_\Sigma - (1 - \eta_A)\eta_F T_a - (1 - \eta_F)T_F}{\eta_F \eta_A} \quad (28)$$

Until now we studied EP as an idealized noise source, not taking the peculiarities of its operation into account. But we faced a number of peculiarities during the EP experimental tests, and these peculiarities are discussed below.

Methods for the EP Noise Properties Test Study

Test Base

Taking into account that the normal operation of plasma source is possible under the environment pressure of no more than 10^{-4} mm Hg, vacuum chambers of different volumes are used for simulating the space environment under ground conditions.

Three types of facilities are currently used for measuring the EP self emission while studying the problems of electromagnetic compatibility:

- Standard anechoic chamber with the thruster mounted inside it, to the nozzle of which a compact vacuum chamber of radio-transparent material (plastic, glass) is connected. This chamber is in its turn connected to the pumping system located outside the anechoic chamber. Electric and magnetic fields produced by the thruster are measured by standard equipment under atmospheric pressure [1];
- Vacuum chamber with the walls covered with radio-absorbing materials (not influencing the vacuum quality), inside which the thruster is mounted. Electric and magnetic fields generated by the thruster are measured inside the vacuum chamber using the specially prepared equipment [3];
- Metal vacuum chamber without the absorbing coatings, inside which the tested EP is mounted. Electric and magnetic fields generated by the thruster are measured in the vacuum medium using the specially prepared equipment [2], [4].

Facilities of the first group allow the most adequate measuring for the characteristics of the thruster self-emission (due to securing the high level of anechoicness), but they require the creation of rather expensive single complex, comprising an anechoic chamber and universal pumping system.

Facilities of the second group solve traditional metrologic task for the measurements inside the anechoic chamber. But under vacuum conditions it is difficult to secure the required anechoicness both due to the absence of broad-band absorbing coatings (overlapping the entire measurement range), and because of the instability of their properties in the vacuum media (intensive outgassing).

Facilities of the third group are the most widely used because of this. In spite of the high level of reflections, these facilities allow rather simple fulfillment of all necessary measurements. Further discussions are continued as applied to them.

Measurement geometry described in [2] and presented in Fig. 6 is used, as a rule. In this case, the thruster is mounted along the axis of vacuum chamber, while the pick-up antennas overlapping the frequency range under study are mounted in the back hemisphere of the thruster at a distance of 1 m from the center of its nozzle (specifications of the electric compatibility measurement standard are used as a basis). It is natural that such measurements do not allow obtaining the comprehensive data on the directivity characteristics for the EP emission.

Methods for Studying the Directivity Characteristics of EP Emission

For obtaining the exhaustive data on spectral characteristics of EP emission, it is necessary to know not only the emission spectral-time response in some definite space part, but its directivity also.

The following test methodology was proposed by the authors for defining the EP emission directivity properties [7]. A thruster and a narrow-directed pick-up antenna (or an array of narrow-directed pick-up antennas overlapping the given frequency range) are mounted along the axis of the cylinder vacuum chamber at a distance L from each other. Symmetry axes of the thruster and pick-up antennas are in the same plane. It is assumed that antennas are provided

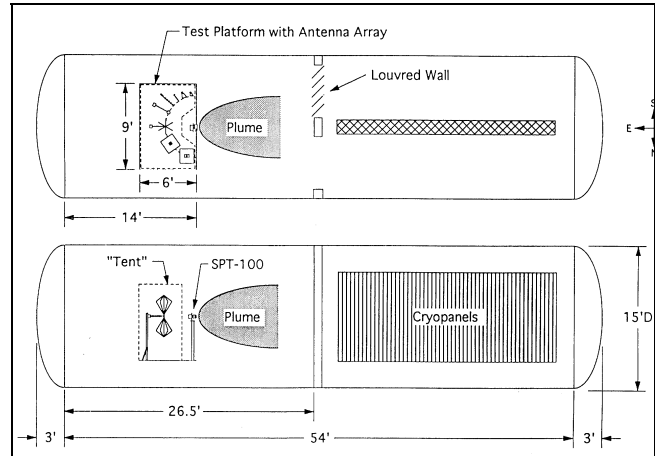


Fig. 6. Vacuum chamber geometry

with the radio-transparent protective shields preventing plasma from direct reaching the apertures.

In the case of one receiving antenna (Fig. 7), its output is connected via the commutator and a set of low-noise amplifiers (overlapping the entire frequency range) to the input of spectrum analyzer SA that provides the noise power measurement at the pick-up antenna output. EP may be rotated remotely about the vertical axis to the angle β (β is an angle between the EP axis and the pick-up antenna axis) within $0 - 180^\circ$. EP rotation in one plane only means axisymmetric character of the EP directivity pattern. While selecting L distance, it is taken into account that the reception of noise signals should be provided in the far zone of the directivity pattern formation both for the antenna and for the emission source.

In view of the directive properties, the power flow density of the EP emission in the observation point is defined by the following expression:

$$\Pi_{TR}(\beta) = \Pi_{OTR} G_{TR}(\beta), \quad (29)$$

where Π_{OTR} - power flow density for the thruster noise averaged over all directions (isotropic) in the

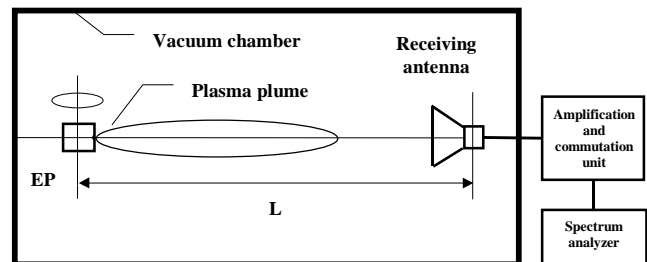


Fig. 7. Test geometry

observation point, $G_{TR}(\beta)$ - directive gain of the thruster noise emission.

$$\Pi_{0TR} = P_{\Sigma} / 4\pi L^2, G_{TR}(\beta) = G_{TRmax} F_{TR}^2(\beta), \quad (30)$$

where $F_{TR}(\beta)$ - normalized thruster emission directivity pattern for the electric field, G_{TRmax} - directive gain in the direction of maximum thruster emission, P_{Σ} - power of noises produced by the thruster.

In this case, power measured by SA at the pick-up antenna output is defined by (17).

The thruster operation starts during the test and its plume axis is rotated by the remote drive within the angle of 0 - 180° relative to the pick-up antenna axis. The current noise power at the pick-up antenna output is measured simultaneously by SA. As is obvious from (30), the readings of power meter will depend only on the function $F_{TR}(\beta)$. Having normalized the measured values to the maximum level, we obtain the normalized directivity pattern of EP emission in power $F_{TR}^2(\beta)$ in the main cross-section. Measurements may be made repeatedly for the other frequency ranges in the case of necessity.

In the case of engineering difficulties connected with providing the thruster rotation, it is possible to use separated reception (Fig. 8). In this case, an array of identical antennas is used, which are located in the same plane and at the same distance L from the thruster center, but under different angles β to its axis. Measurements obtained in the main cross-sections may be generalized to the case of spatial directivity pattern, if the latter is the body of rotation.

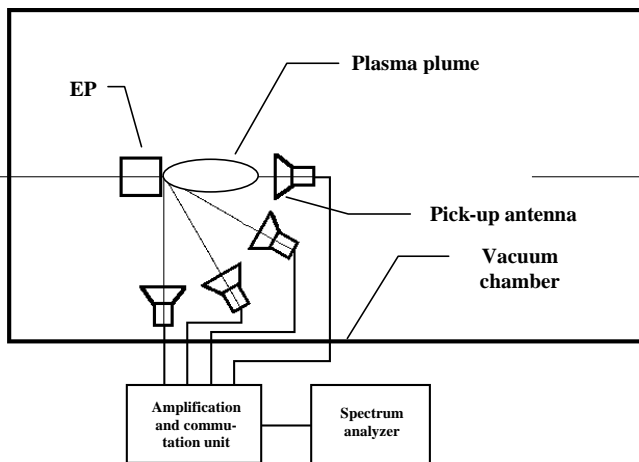


Fig.8. Test geometry

If there are doubts on the presence of asymmetry in the EP emission directivity pattern (due to the location of cathode-compensator near the thruster exit plane, for example), then using the proposed methods it is possible to study the directivity pattern not in the main cross-sections only, but for the arbitrary angles of view also.

Thus, the developers of on-board radio systems have a possibility now to take into account the real mutual location of EP and receiving antennas from the point of view of their noise influence.

EP Equivalent Noise Temperature Measurement Methods

Let's confirm (13) for the case when narrow pick-up antennas with low level of side lobes are used. One may consider that within the main lobe of antenna directivity pattern the distribution function of EP equivalent noise temperature varies slowly in the antenna environment, and $T(\theta, \varphi)$ may be brought out of the integral sign. In the spherical coordinate system connected with EP, taking into account that:

$$\int_{4\pi} D(\theta, \varphi) \sin \theta d\theta d\varphi = 4\pi, \quad (31)$$

we obtain: $T_{TRI} = T(L, \beta_0, \gamma_0)$, where: β, γ - spherical angular coordinates with the sphere center in the point of thruster location (β_0, γ_0 - angular directions to the point of measurements), L - distance from EP to the point of measurements.

Expression for the spatial distribution function for the EP equivalent noise temperature $T(L, \beta, \gamma)$ in view of (30) may be converted to the following form:

$$T(L, \beta, \gamma) = T_{TRmax}(L) \cdot F^2(\beta, \gamma), \quad (32)$$

where $T_{TRmax}(L)$ - maximum effective noise temperature of EP at L distance.

If we measure $T_{TRmax}(L)$ at distance $L = L_0$, it is not difficult to calculate $T_{TRmax}(L)$ for any L value:

$$T_{TRmax}(L) = T_{TRmax}(L_0) \frac{L_0^2}{L^2} \quad (33)$$

Thus, the measurement task is reduced to measuring $T_{TRmax}(L_0)$ and defining the normalized directivity pattern of EP in power $F^2(\beta, \gamma)$.

These measurements have definite specifics, so let's study them in more details. Test geometry presented in

Fig. 7 is used as a basis. Using the EP rotation and a stable pick-up antenna, it is possible to define the normalized directional pattern of EP in power in the main cross-section $F^2(\beta)$ (for axisymmetric case).

It is possible to use block-diagram presented in Fig. 5 for measuring the EP noise temperature. In this case, pick-up antenna is mounted inside the vacuum chamber at distance $L = L_0$ from EP, and by a sealed adapter and cable it is connected to the reception path and measuring receiver. Reception path, measuring receiver, and standard noise generator are mounted outside the vacuum chamber.

Total equivalent noise temperature at the output of the measuring antenna feeder T_{Σ} is measured by the above methods. Measurements are made when the thruster is “OFF” - $T_{\Sigma 1}$ and “ON” - $T_{\Sigma 2}$. In the first case $T_{\Sigma 1}$ defines the noise emission of metal vacuum chamber that may be characterized by T_T – the equivalent noise temperature of the metal vacuum chamber in the pick-up antenna aperture. Final definition of the EP equivalent noise temperature T_{TRI} in the pick-up antenna aperture is made using (28), where T_{Σ} must be substituted by $T_{\Sigma 2} - T_{\Sigma 1}$. From all T_{TRI} measurements within $\beta = 0 - 180^\circ$ the maximum one should be selected that corresponds to the desired value $T_{TRmax}(L_0)$.

Potential accuracy of the described measurements is defined both by the level of interfering reflections from the metal vacuum chamber walls (the degree of anechoicness), and by acceptability of the assumption on the “narrowness” of directivity pattern and low level of the pick-up antenna side lobes. Taking into account that when the pick-up antenna is placed into the metal vacuum chamber, its directivity pattern may change uncontrollably, it is advisable to use the method of through calibration of the measuring section. It is necessary for this to place the source of the standard noise signal with the known equivalent noise temperature into the aperture of pick-up antenna mounted inside the vacuum chamber. It is the most easy to use a temperature radiating source, an analog of “absolutely black body”, for which the test dependence of its effective noise temperature on real physical one is known, as a standard source. In practice, such sources are made on the basis of distributed matched absorbers, coupled electrically

with antennas under calibration. Functional diagram of measurements for the case of using a temperature radiating source as a standard is presented in Fig. 9. As it was in the previous case, pick-up antenna, connected by a cable to the outer measuring complex, is mounted inside the vacuum chamber only. Standard absorber, the shape and size of which are chosen proceeding from securing the maximum screening for the antenna aperture against the influence of spurious heat sources located in the working zone of the vacuum chamber, is placed into the pick-up antenna aperture.

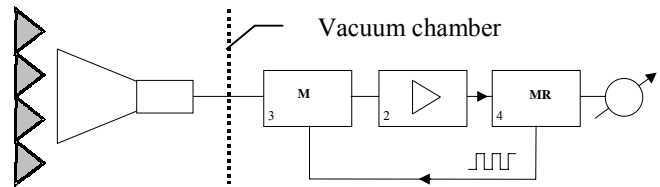


Fig.9.

During the calibration, measuring receiver 4 controls the modulator 3 and the output signal of the meter is proportional to the equivalent noise temperature T_G of the standard source that is known. During the measurement process, the standard source is removed from the antenna aperture, and the output signal is proportional to the equivalent noise temperature T_{Σ} . Having defined the ratio of signals obtained while making measurements and calibration, we come back to the formula (26) for the case $T_{RT}=0$. For the due account for the equivalent noise temperature of the chamber T_T , measurements are made for the modes of operating and non-operating EP with subsequent account for T_T in calculations. The procedure of $T_{TRmax}(L_0)$ measurement repeats the described above.

If the calibrated heat radiating source is not available to the researches making this test, they may calibrate it themselves. For this, facility, corresponding to the presented in Fig. 5, is mounted inside the antenna hall, and a fragment of vacuum-resistant radio-absorbing coating of required size with the known equivalent noise temperature, for example, is placed into the pick-up antenna aperture at a fixed known distance. Using a standard noise generator 1, it is easy to calibrate the selected source in the units of noise temperature. It is advisable to broaden measurements to the range of possible physical temperatures of the selected source for obtaining the interconnection

between the equivalent noise temperature and the physical one.

Thus, using the proposed measurement methods, it is possible to obtain comprehensive noise characteristics of EP within the frames of spatial distribution of noise temperature. If $L_0=1$ m in (33) (electromagnetic compatibility standard), the EP equivalent noise temperature in any point of space is defined by the following expression:

$$T(L, \beta, \gamma) = \frac{T_{TRO}}{L^2} F^2(\beta, \gamma), \quad (34)$$

where T_{TRO} is the maximum effective noise temperature of EP at a distance of 1 m.

The expression (34) is valid for exact central frequency and bandwidth of the measuring receiver, which should be put into correspondence with the similar characteristics of the real reception path under study.

While assessing the real sensitivity of the reception path in the operating thruster emission, it may appear that the required minimum sensitivity is not reached. In this case, the problem may be solved by two ways:

- Optimization of the mutual location of receiving antennas and EP taking into account the exact form of the EP emission directivity pattern $F(\beta, \gamma)$;
- Introduction of corresponding limitation to the level of noises, reaching the bandwidth of the reception path, into the EP specification. Ultimate T_{TRO} values should be given in the specification for all critical frequency ranges using the terms of (34).

Conclusion

Studying the radio channel and EP as a single electrodynamic system, authors made a comprehensive analysis for the noise properties of typical radio-reception paths and antenna feeder devices. Noise factor and equivalent noise temperature were used as parameters characterizing the sensitivity of radio-reception path. It is shown that the EP noise influence is mainly defined by the level of additional noises coming to the reception path input at the operating EP. Potential boundaries of the typical radio link noise immunity at a presence of operating EP are defined in the paper.

On the basis of the analysis made, authors have

elaborated a new universal approach to the description of EP noise properties, based on the representation of EP as an equivalent noise source with the known spatial distribution of equivalent noise temperature. Such approach allows unambiguous calculation for the real sensitivity of the reception path at any mutual orientation of the reception antennas and EP, but requires fulfillment of preliminary complex measurements. So, special attention was paid by the authors in the paper to the problems of test study of both EP noise characteristics under ground conditions, and noise characteristics of typical radio-reception paths. For assessing the noise characteristics of real EP within the frames of used models, authors have proposed a number of new original test procedures based on fulfilling radio-physical measurements inside the typical metal vacuum chambers.

As a result of studies, recommendations are given for the optimization of parameters not for the radio channels only, but for EP also for securing the allowable emission power levels (which should be given in the specification in addition to the EMC standards) within the ranges of operation of onboard radio-reception paths. The latter is especially actual while designing the super-far links for the space radio communications with interplanetary spacecrafts equipped with sustainer propulsion systems based on electric propulsions.

The practical value of the results obtained is in the possibility to develop new engineering procedures and methods allowing to conduct systematic designing of onboard radio-engineering complexes operating in active interferences produced by electric propulsions.

References

- [1] S. Kitamura, "Development of the Engineering Test Satellite-3 (ETS-3) Ion Engine System," *NASA TM-77538*, 1984.
- [2] L.H. Caveni, F.M. Curran, J.R. Brophi, "Russian Electric Space Propulsion Evaluated for Use on American Small Satellites," *2nd German-Russian Electric Propulsion Conference*, Moscow, Russia, July 1993.
- [3] V. Kim, A. Plokhikh, A. Sorokin, and A. Solomatin, "Methods and Means for Studying the Hall Thrusters Self-Radiation," *2nd German-Russian Electric Propulsion Conference*, Moscow, Russia, July 1993.

[4] A.P. Plokhikh, N.A. Vazhenin, C.J. Sarmiento, and J.M. Sankovic "Study of the Hall Thruster Self-Emission Effective Center Location Within the Radio Frequency Band," *25th International Electric Propulsion Conference*, Cleveland, Ohio, August 1997.

[5] Gennady G. Shishkin, Andrey P. Plokhikh, "Analysis of Electromagnetic Emission of Plasma Injectors," *XIII International Conference on Gas Discharges and Their Applications*, Glasgow, UK, September 2000.

[6] K.I. Almazov-Dovzhenko, "Noise Factor and Its Measurement in Microwaves," *Nauchny mir*, Moscow, 2000 – in Russian.

[7] A.P. Plokhikh, N.A. Vazhenin, G.V. Soganova, "Methods for Investigating the Spectrum Characteristics of Emission for the Plasma Flows of Artificial Origin Injected in the Ionosphere of Earth," *International Geoscience and Remote Sensing Symposium*, Sydney, Australia, 9-13 July, 2001.